Development 128, 3609-3621 (2001)
Printed in Great Britain © The Company of Biologists Limited 2001
DEV3440

Mouse embryos lacking Smad1 signals display defects in extra-embryonic tissues and germ cell formation

Kimberly D. Tremblay, N. Ray Dunn and Elizabeth J. Robertson*

Molecular and Cellular Biology, Harvard University, 16 Divinity Avenue, Cambridge, MA 02138, USA
*Author for correspondence (e-mail: ejrobert@fas.harvard.edu)

Accepted 21 June 2001

SUMMARY

The Smad proteins are important intracellular mediators of the transforming growth factor β (TGFβ) family of secreted growth factors. Smad1 is an effector of signals provided by the bone morphogenetic protein (BMP) subgroup of TGFβ molecules. To understand the role of Smad1 in mouse development, we have generated a Smad1 loss-of-function allele using homologous recombination in ES cells. Smad1–/– embryos die by 10.5 dpc because they fail to connect to the placenta. Mutant embryos are first recognizable by 7.0 dpc, owing to a characteristic localized outpocketing of the visceral endoderm at the posterior embryonic/extra-embryonic junction, accompanied by a dramatic twisting of the epiblast and nascent mesoderm. Chimera analysis reveals that these two defects are attributable to a requirement for Smad1 in the extra-embryonic tissues. By 7.5 dpc, Smad1-deficient embryos show a marked impairment in allantois formation. By contrast, the chorion overproliferates, is erratically folded within the extra-embryonic space and is impeded in proximal migration. BMP signals are known to be essential for the specification and proliferation of primordial germ cells. We find a drastic reduction of primordial germ cells in Smad1-deficient embryos, suggesting an essential role for Smad1-dependent signals in primordial germ cell specification. Surprisingly, despite the key involvement of BMP signaling in tissues of the embryo proper, Smad1-deficient embryos develop remarkably normally. An examination of the expression domains of *Smad1*, *Smad5* and *Smad8* in early mouse embryos show that, while *Smad1* is uniquely expressed in the visceral endoderm at 6.5 dpc, in other tissues *Smad1* is co-expressed with *Smad5* and/or *Smad8*. Collectively, these data have uncovered a unique function for Smad1 signaling in coordinating the growth of extra-embryonic structures necessary to support development within the uterine environment.

Key words: Smad1, Extra-embryonic tissues, Primordial germ cells, BMP, Mouse

INTRODUCTION

The earliest differentiation events during mammalian development reflect the necessity of the embryo to survive in the uterine environment and involve the formation of extra-embryonic tissues, which have a crucial role in supporting development but do not contribute to the resulting animal. At early post-implantation stages, the mouse embryo comprises three cell lineages: the extra-embryonic ectoderm, which gives rise to the placenta and the ectodermal component of the chorion, the primitive endoderm, which forms the endoderm of the parietal and visceral yolk sacs, and the epiblast, which gives rise to the embryo proper. The process of gastrulation converts the epiblast into the three definitive germ layers of the embryo, as well as generating the extra-embryonic mesoderm that participates in the formation of the visceral yolk sac (VYS), amnion, chorion and allantois. Thus, the development of the embryo within the uterine environment requires the coordinate growth and morphogenesis of both the embryonic and extra-embryonic tissues.

Inductive interactions between the tissue layers of the early embryo govern formation of the early body plan and control numerous processes, including cell proliferation, differentiation and migration (Beddington and Robertson, 1999). Members of the transforming growth factor β (TGFβ) family of growth factors regulate many of these aspects of post-implantation development (Goumans and Mummery, 2000). TGFβ ligands can be divided into two groups in accordance with biological and structural criteria: BMP/GDF and TGFβ/activin/nodal (Kingsley, 1994). Experiments in the mouse have underscored the diverse roles these classes of molecules play during development. Chimera analysis and loss-of-function studies have shown that nodal signaling is important in guiding the formation of both the anteroposterior (AP) and left-right axis (Schier and Shen, 2000). Loss of BMP4 function results in gastrulation defects, with many embryos failing to form sufficient mesoderm (Winnier et al., 1995). Those embryos surviving beyond gastrulation display truncated and disorganized posterior structures, including extra-embryonic mesoderm derivatives and entirely lack primordial germ cells (PGCs) (Lawson et al., 1999; Winnier et al., 1995). Similarly, loss of BMP2 function also disturbs early developmental processes and causes defective development of the amnion, chorion, and heart, implicating BMP2 in the formation of

both extra-embryonic and embryonic mesodermal derivatives (Zhang and Bradley, 1996).

TGFβ ligands signal via heteromeric complexes composed of type I and type II cell-surface serine/threonine kinase receptors (Massague, 1998). In the ligand-induced complex, the type II receptors phosphorylate and activate type I receptors. Activated type I receptors in turn phosphorylate Smad family members, which constitute the only known substrates of the type I receptors (Massague, 1998). To date, nine mammalian Smads have been identified, which fall into three classes based on biological and structural criteria: pathway-specific Smads, common Smads and inhibitory Smads (reviewed by Whitman, 1998). Thus, in response to TGFβ-mediated signaling the pathway-specific Smads, including Smad1, 2, 3, 5 and 8, are selectively phosphorylated at their C termini by specific type I receptors. Once phosphorylated, the pathway-specific Smads complex with the common Smad, Smad4, and translocate into the nucleus where, via interaction with DNA-binding proteins such as OAZ and FAST, they direct specific transcriptional responses (Wotton et al., 1999). Considerable biochemical and embryological evidence has shown that the pathway-specific Smads act as the intracellular mediators for distinct classes of ligands. Smad2 and Smad3 are phosphorylated by the TGFβ type I and activin type IB receptors (Macias-Silva et al., 1996; Zhang et al., 1996), whereas Smad1, Smad5 and Smad8 are activated by BMP type I receptors (Hoodless et al., 1996; Kawai et al., 2000; Nishimura et al., 1998). Moreover in *Xenopus* animal cap assays, *Smad2* induces dorsal mesoderm in a manner similar to overexpression of *activin* and *nodal* (Graff et al., 1996; Suzuki et al., 1997), whereas *Smad1* and *Smad5* causes formation of ventral mesoderm, a response evoked by *Bmp2* and *Bmp4* (Baker and Harland, 1996; Graff et al., 1996).

Given the high degree of homology shared by members of the Smad family, it has been of interest to understand the extent to which they function interchangeably in vivo. The function of Smad proteins has been addressed in the mouse using gene targeting approaches and has shown that highly related Smad proteins can have diverse roles in the normal animal. Thus, Smad2 plays a central role in AP axis formation and *Smad2*-deficient embryos are abnormal at gastrulation (Heyer et al., 1999; Nomura and Li, 1998; Waldrip et al., 1998; Weinstein et al., 1998), ultimately forming only extra-embryonic mesoderm derivatives. By contrast, despite sharing 92% amino acid identity with Smad2, *Smad3*-deficient mice show only impaired immune functions and a predisposition to colon cancer (Yang et al., 1999b; Zhu et al., 1998). As yet, it is unclear whether the differences in phenotype are due to distinct responses mediated by either Smad or whether they are reflective of their unique expression patterns.

To date, the role of only a single BMP-specific Smad, Smad5, has been studied in the mouse. *Smad5* mutants die by 10.5 dpc and display multiple embryonic and extra-embryonic phenotypes, including gut, cardiac and laterality defects, as well as increased mesenchymal apoptosis, and lack of forebrain tissue (Chang et al., 1999; Chang et al., 2000; Yang et al., 1999b). These defects are consistent with a generalized abrogation of BMP signaling; however, the relatively late onset of these phenotypes, in comparison with those observed for *Bmp2* and *Bmp4* mutations, suggests that other BMP-regulated Smads such as Smad1 or Smad8 must contribute in transducing BMP signals during early embryogenesis.

In the present study, we have explored the role of Smad1, a second member of the BMP signaling pathway, in the mouse. Similar to *Smad5* mutants, *Smad1*$^{-/-}$ embryos die at 10.5 dpc. However the phenotypes of the two mutations are largely non-overlapping. Thus, unlike *Smad5*$^{-/-}$ embryos, loss of Smad1 does not prevent the formation and patterning of the embryo proper. Rather, from early post-gastrulation stages onwards, *Smad1* mutants exhibit pronounced defects in the morphogenesis and proliferation of extra-embryonic tissues, which collectively result in embryonic lethality. These defects include overgrowth of the posterior visceral endoderm (VE), as well as the extra-embryonic ectoderm and mesoderm of the chorion. Surprisingly, loss of Smad1 has the opposite growth effect on the allantois, leading to a dramatic reduction in the size and patterning of this tissue and concomitant failure to form the umbilical connection to the placenta. In addition *Smad1*-deficient embryos display a marked reduction in the number of primordial germ cells (PGCs) at 8.5 dpc. Thus, our data demonstrate that Smad1 pathways play a pivotal role in controlling the proliferation and morphogenesis of the extra-embryonic tissues during early mammalian development.

MATERIALS AND METHODS

Mutagenesis of the Smad1 locus

A 129/SvJ mouse genomic library (Stratagene) was screened with a full-length Smad1 cDNA clone and three independent λ clones containing the first coding exon were identified. To generate the Smad1^{Robm1} construct, a PGK-neo selection cassette was inserted between a 2.8 kb *Pst*I/*Bam*HI 5′ sub-fragment and a 5.1 kb 3′ *Hin*dIII sub-fragment. Fifteen micrograms of *Cla*I linearized vector was electroporated into 2×10^7 CCE ES cells (Robertson et al., 1986). DNA from drug-resistant clones was digested with *Eco*RI and screened by Southern blot hybridization using two external probes: a 0.8 kb *Sal*I/*Pst*I 5′ probe and a 0.6 kb *Hin*dIII/*Eco*RI 3′ probe. Four of 600 G418-resistant clones were correctly targeted, one of which was injected into C57Bl/6J blastocysts. Germline chimeras were crossed to MF1 females (Harlan) and the resulting heterozygous offspring intercrossed or further bred to MF1 females.

The Smad1^{RobPC} allele was generated by inserting a loxP and *Eco*RI site into the *Stu*I site of the 4.5 kb *Eco*RI/*Bam*HI 5′ arm. The 3′ arm was constructed by inserting a loxP-flanked PGK-hygro cassette into the *Mlu*I site of the 5.8 kb *Bam*HI/*Hin*dIII fragment. A 3′ MCI-tk cassette was added. Drug-resistant ES-cell clones were screened by Southern blot using a 3′ external probe (as above) and an internal hygro probe. Three of 700 clones were correctly targeted and two were used to produce germline chimeras. Heterozygous Smad1^{RobPC} mice were mated to mice carrying a Protamine-Cre transgene (O'Gorman et al., 1997). Heterozygous males carrying the transgene were mated to MF1 females. Because Cre-mediated recombination leads to three potential configurations of the Smad1^{RobPC} locus, the progeny were screened by Southern blot analysis. *Eco*RI- and *Bam*HI-digested tail DNA samples were probed with the 3′ external probe, hygro probe and 5′ internal probe to identify animals carrying the Smad1^{Robcn} allele.

For both *Smad1* alleles, embryos from 9.5 dpc onwards were genotyped by Southern blot analysis of yolk-sac DNA. Younger embryos derived from *Smad1*^{Robm1} heterozygous intercrosses were genotyped by PCR with the *Smad1*-specific primers 5′-GTCGAACAGTGTACGCCAAGC-3′ and 5′-CCTGTTTCCACCC-AAGGAGTC-3′, and with *neo*-specific primers 5′-CGTCTGATGCC-GCCGTGTTCC-3′ and 5′-CTTCGCCCAATAGCAGCCAGTCC-3′.

Northern and western blot analysis

Total RNA was extracted from individual 9.5 dpc embryos using the TRIzol method (Gibco/BRL). Fifteen micrograms of total RNA were size fractionated on a 1.3% agarose-formaldehyde gel, transferred onto GeneScreen Plus (NEN Research Products), and probed with a ^{32}P random-primed 700 bp *Eco*RI/*Hin*dIII fragment, comprised mostly of *Smad1* 3′ UTR. For Western blot, embryos or COS cells, were lysed in sample buffer (0.0625 M Tris-HCL, pH 6.8, 2.0% SDS, 5.0% 2-mercaptoethanol, 0.002% Bromophenol Blue, 10.0% glycerol) and sonicated. Lysates (20 μg) were fractionated by SDS-PAGE using 12% separating gels, transferred onto nitrocellulose and membranes incubated overnight with an anti-Smad1 antibody (Upstate, 1:500) that recognized amino acids 147-258 of human Smad1. The secondary antibody was a bioatinylated goat anti-rabbit IgG (ICN, 1:150,000). Finally, filters were incubated with streptavidin/HRP conjugate (Phar Mingen, 1:1000) and HRP detected using an ECL kit (Amersham, IL).

Histology and in situ hybridization

Embryos were fixed in 4% paraformaldehyde (PFA) in phosphate-buffered saline (PBS) at 4°C overnight, followed by dehydration through a graded ethanol series. Embryos were cleared in xylene, embedded in Fibrowax (BDH Laboratory Supplies, England) and sectioned at 8μm. Sections were collected on Tespa-treated glass slides and stained with Hematoxylin and eosin using standard procedures.

Whole-mount in situ hybridization was performed as described (Wilkinson, 1992). Antisense probes specific for *AFP* (Waldrip et al., 1998), *Sox2* (Conlon et al., 1994), *T* (Wilkinson et al., 1990), *eomesodermin* (Russ et al., 2000), *Bmp4* (Jones et al., 1991), *Fgf8* (Crossley and Martin, 1995) and *Fgf4* (Wilkinson et al., 1988) were used as described. Embryos were post-fixed in 4% PFA, photographed, dehydrated in ethanol, cleared in xylenes, embedded in paraffin and sectioned at 8 μm. Sections were dewaxed using standard procedures, mounted in Cytoseal and photographed using Normarski optics.

Radioactive in situ hybridization was performed as described (Jones et al., 1991). The probes used include a full-length *Smad1* (Waldrip et al., 1998) and the proline-rich linker domain of *Smad5* (Meersseman et al., 1997). The *Smad8* probe is a 437 bp clone that corresponds to the linker region (kindly provided by G. Chu). Sections were photographed using a Leitz DMR microscope and Fugichrome Velvia color slide film.

Visualization of PGCs

Primordial germ cells were visualized and counted according to Lawson et al. (Lawson et al., 1999). Genotype was assessed by PCR analysis of yolk-sac DNA.

Generation and analysis of chimeric embryos

Blastocysts, recovered from *Smad1^{Robm1}* intercrosses were injected with 10-15 wild-type KT4 ES cells (Tremblay et al., 2000). After transfer into pseudopregnant foster females, the manipulated embryos were recovered at 7.5 dpc, fixed and stained for β-galactosidase activity.

RESULTS

Targeted Disruption of the murine *Smad1* gene

Two independent targeting constructs were designed to mutate the first coding exon of *Smad1*. One vector replaces most of this exon and 30 bp of 3′ flanking sequence with a neomycin-resistance cassette (Fig. 1A). Because homologous recombination leads to deletion of the initiation codon and sequences encoding most of the MH1 domain, the resulting mutation is predicted to generate a null allele. A single correctly targeted ES cell clone was used to generate chimeras that transmitted the mutation, termed *Smad1^{Robm1}*, to progeny. A second null allele was generated by in vivo Cre-mediated excision of a conditional allele, *Smad1^{RobPC}* (Fig. 1B). The conditional allele harbors an *Eco*RI and *loxP* site inserted 5′ and a *loxP*-flanked hygromycin-resistance cassette inserted 3′ of the first coding exon. Two independently targeted ES-cell clones were used to generate chimeras. Offspring carrying the *Smad1^{RobPC}* allele were mated to mice carrying a Protamine-Cre transgene that directs Cre-recombinase expression specifically to the male germline (O'Gorman et al., 1997). Thus, germline recombination results in one of several configurations of the *Smad1* locus, including the null allele termed *Smad1^{Robcn}* (Fig. 1B). The *Smad1^{Robcn}* allele removes all of the first coding exon and approximately 2 kb of 5′ and 3′ flanking genomic sequences, but leaves a single *loxP* and *Eco*RI site in the locus (Fig. 1B).

Northern blot analysis of RNA isolated from homozygous mutant embryos demonstrated that the *Smad1^{Robm1}* and *Smad1^{Robcn}* mutations result in the production of a truncated transcript (Fig. 1E). To determine if the remaining transcript encodes a protein, Western blot analysis was performed on individual 9.5 dpc embryos with an antibody that recognizes the C-terminal domain of Smad1 (Fig. 1F). Although a band of approximately 55 kDa was detected in wild-type and heterozygous samples, neither a wild-type nor a smaller form of Smad1 protein were present in homozygous mutant embryos, confirming that both alleles produce null mutations.

Loss of Smad1 results in embryonic lethality by 10.5 dpc

Although *Smad1* heterozygous mice were normal and fertile, no live born *Smad1^{Robm1}* or *Smad1^{Robcn}* homozygous mice were produced from heterozygous matings (Table 1), and both alleles result in identical embryonic lethal phenotypes. Timed matings from heterozygous intercrosses were used to determine the onset of lethality. With death described as the presence of necrotic cells and lack of a beating heart, *Smad1*-null embryos were dead or dying by 10.5 dpc and failed to establish a functional placental connection. Because other mutations with defects in placentation also die at a similar developmental stage (Gurtner et al., 1995; Kwee et al., 1995; Luo et al., 1997; Yang et al., 1995), the lethality of the *Smad1* mutation is likely attributable to this defect.

Table 1. Phenotype and genotype of offspring from Smad1 heterozygous intercross

	Phenotype		Genotype			
Age	Normal	Abnormal*	+/+	+/–	–/–	Total
7.5 dpc‡	114	38 (25%)				152
8.5 dpc‡	131	51 (28%)				182
9.5 dpc	142	43	44	98	43 (23%)	185
10.5 dpc	29	10§	11	18	10 (26%)	39
11.5 dpc	24	5¶	9	15	5 (20%)	29
13.5 dpc	26	3¶	11	15	3 (10%)	29
Neonates			82	172	0	254

*Phenotype includes posterior folds and abnormal allantois.
‡Embryos not genotyped.
§Number includes dying embryos.
¶Number includes necrotic embryos or absorptions.

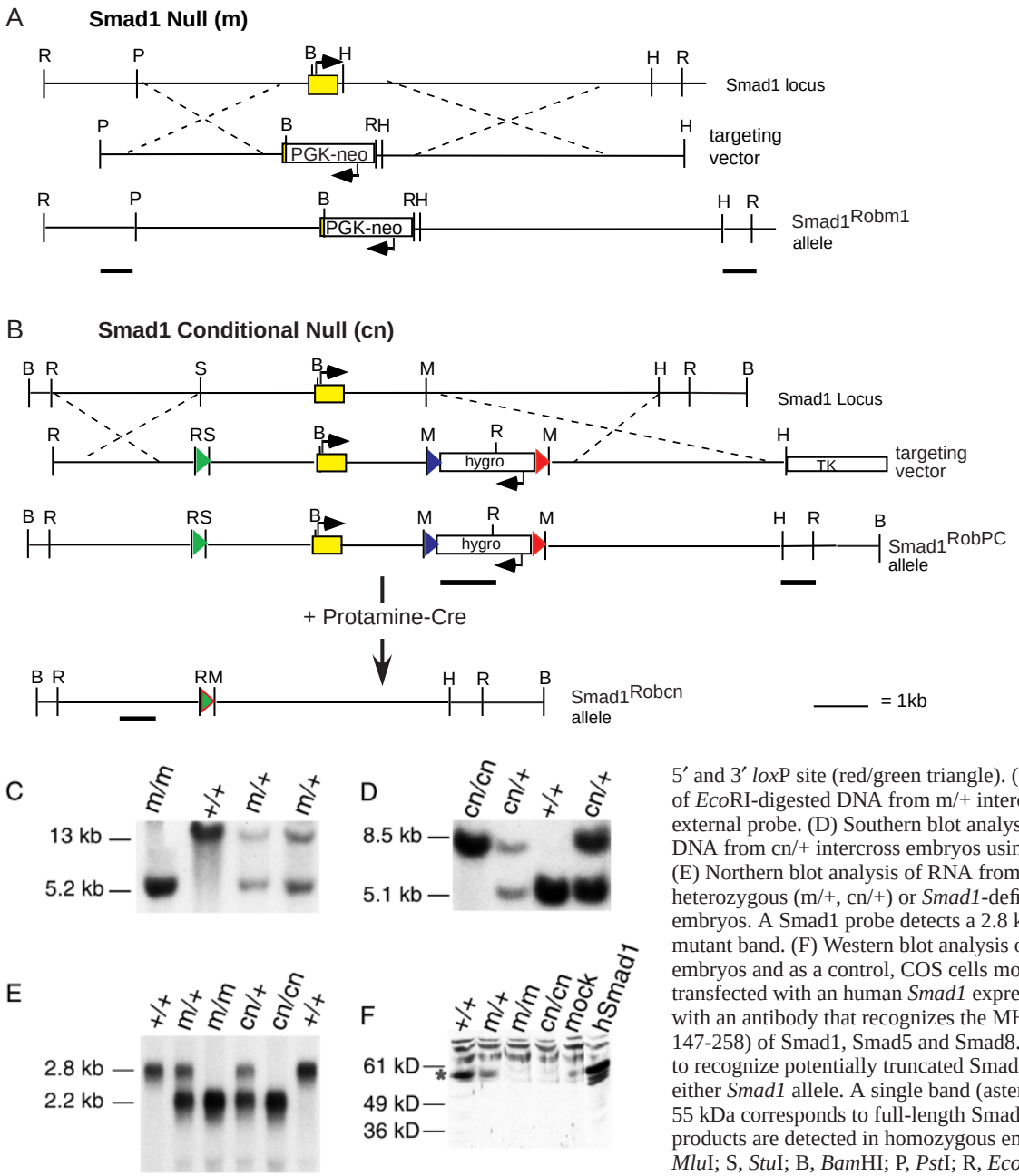

Fig. 1. Generation of *Smad1*-deficient mice. (A,B) Targeting strategies. Thick lines represent Southern probes and arrows the direction of transcription. (A) The *Smad1*^{Robm1} (m) vector replaces most of the first coding exon (yellow box) and 30 bp of 3′ flanking sequence with a PGK-*neo* cassette. (B) The *Smad1*^{RobPC} vector introduces an *Eco*RI (R) and *loxP* site (green triangle) 2 kb 5′ of the first coding exon and a *loxP*-flanked (blue and red triangles) *hygro* cassette 1.7 kb 3′ of the exon. Germline Cre-mediated excision of the *Smad1*^{RobPC} allele was used to produce the *Smad1*^{Robcn} (cn) allele, which retains part of the 5′ and 3′ *lox*P site (red/green triangle). (C) Southern blot analysis of *Eco*RI-digested DNA from m/+ intercross embryos using the 5′ external probe. (D) Southern blot analysis of *Bam*HI-digested DNA from cn/+ intercross embryos using the 5′ internal probe. (E) Northern blot analysis of RNA from wild-type (+/+), *Smad1* heterozygous (m/+, cn/+) or *Smad1*-deficient (m/m, cn/cn) 9.5 dpc embryos. A Smad1 probe detects a 2.8 kb wild-type and a 2.2 kb mutant band. (F) Western blot analysis of individual 9.5 dpc embryos and as a control, COS cells mock transfected or transfected with an human *Smad1* expression construct and probed with an antibody that recognizes the MH2 domain (amino acids 147-258) of Smad1, Smad5 and Smad8. This antibody is predicted to recognize potentially truncated Smad1 proteins produced from either *Smad1* allele. A single band (asterisk) of approximately 55 kDa corresponds to full-length Smad1. No intact or truncated products are detected in homozygous embryos. H, *Hind*III; M, *Mlu*I; S, *Stu*I; B, *Bam*HI; P, *Pst*I; R, *Eco*RI.

Gastrulation defects in *Smad1* mutant embryos

The first morphological abnormalities in *Smad1*-deficient embryos coincide with the onset of gastrulation. Although gastrulation appears to initiate normally, as evidenced by the formation of a primitive streak and emergence of nascent mesoderm, characteristic ruffles are present in the VE overlying the distal extra-embryonic region adjacent to the primitive streak (Fig. 2A,B,D). Despite the grossly abnormal shape of the posterior VE, the individual cells within the ruffles display the columnar/cuboidal morphology characteristic of extra-embryonic VE and also maintain proper cell-cell adhesion.

The second visible abnormality is a profound distortion of the embryonic region. Although wild-type embryos are bilaterally symmetric along the proximodistal (PD) axis, whole-mount and histological analyses reveals that this symmetry is rarely maintained in *Smad1*-mutant embryos. The epiblast and newly formed mesoderm display an abnormal twisting that is evident by 7.0 dpc (Fig. 2C,E). In spite of these profound morphological defects, *Smad1*-deficient embryos proceed through gastrulation and are represented at Mendelian ratios at 9.5 dpc (Table 1). Although the VE invariably remains ruffled at 8.0-8.5 dpc, the emerging AP axis is symmetrical, headfolds and somites form, gross VYS morphology and accompanying mesoderm are normal, and the node is clearly defined (Fig. 2I,J).

Defects in extra-embryonic ectoderm and mesoderm formation

At the onset of gastrulation, epiblast cells move towards and ingress through the primitive streak to form mesoderm. Fate-

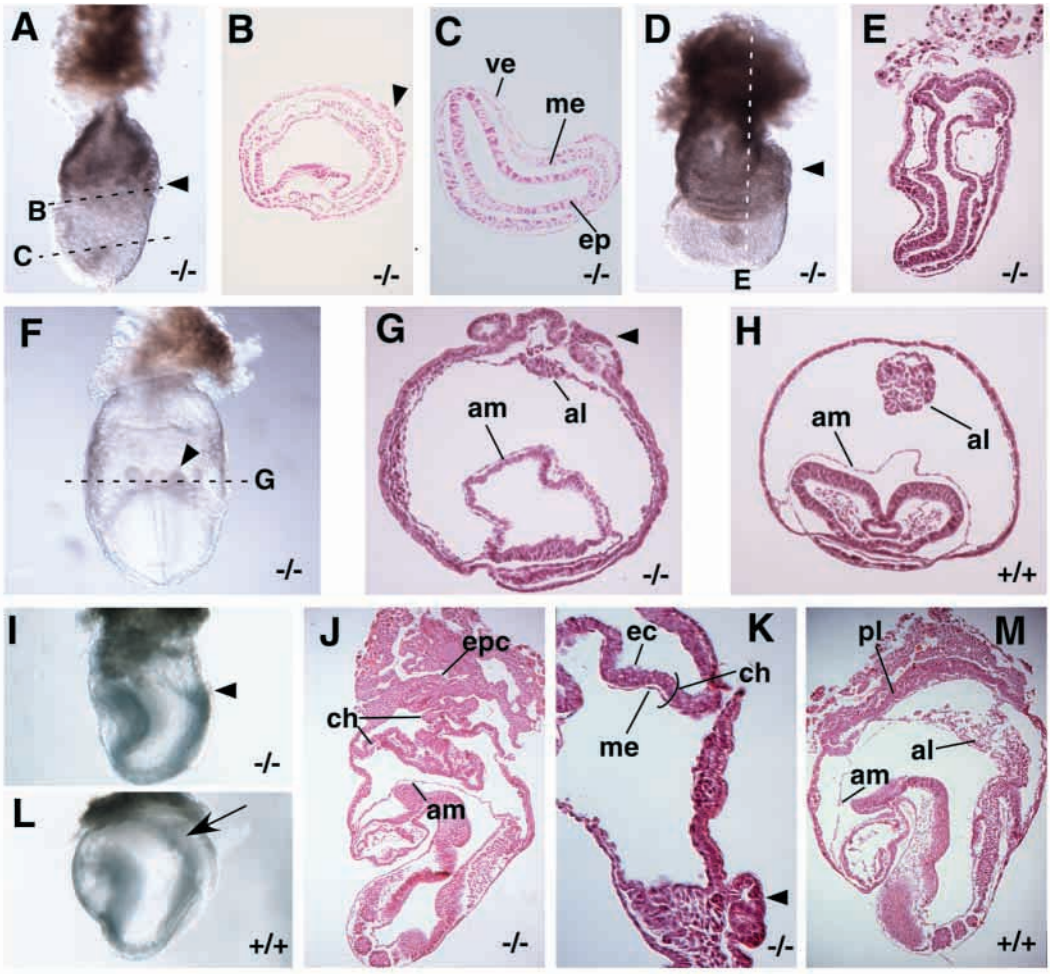

Fig. 2. Gastrulation and extra-embryonic defects in *Smad1*-deficient embryos. (A) At 7.0 dpc, *Smad1* mutant (–/–) embryos develop characteristic folds (arrowhead in all panels) in the extra-embryonic region proximal to the primitive streak. (B) A transverse section through the extra-embryonic region of the embryo in A reveals folding of the VE, while more distally (C), all three tissue layers are abnormally twisted. (D) *Smad1* mutant embryos at 7.5 dpc demonstrate characteristic folds. (E) A frontal section of the embryo in D showing extensive twisting of the epiblast. (F) Posterior view of early headfold mutant embryo (8.0 dpc) showing lack of a recognizable allantoic bud. (G) In a transverse section through the embryo in F, a small allantoic rudiment is evident. (H) By contrast, a transverse section through an age matched wild-type (+/+) littermate reveals extensive growth of the allantois. (I) By 8.5 dpc, mutant embryos show a normal AP axis, but extra-embryonic tissues are abnormal. (J) In sagittal section, an 8.5 dpc mutant embryo has an erratically folded chorion and lacks an extended allantois. (K) A magnified view of a sagittal section through the posterior folds of the embryo in I demonstrates that the extra-embryonic mesoderm has migrated properly to line the entire exocoelomic surface of the chorionic ectoderm and visceral yolk sac. (L) By contrast, in wild-type littermates an elaborated allantois is evident (arrow), that in sagittal section (M) is fused with the chorion to produce a placenta. (A-D,I-L) anterior is towards the left. al, allantois; am, amnion; ch, chorion; ec, ectoderm; ep, epiblast; epc, ectoplacental cone; me, mesoderm; pl, placenta; ve, visceral endoderm.

mapping studies have shown that precursors of the extra-embryonic mesoderm are located in the proximal portion of the epiblast and are the first cell population to traverse the streak (Lawson et al., 1991). Extra-embryonic mesoderm emerges as a bulge of tissue that displaces the overlying extra-embryonic ectoderm. This bulge of cells, together with a slower growing anterior bulge, cavitates to form the posterior and anterior amniotic folds. These folds eventually fuse, forming a physical barrier between the embryo proper and the extra-embryonic tissues. A second consequence of this proximal migration of extra-embryonic mesoderm is the displacement of the extra-embryonic ectoderm, the precursor of the chorion that overlies the epiblast. These coordinated morphogenetic movements lead to the emergence of the chorion as a distinct anteriorly tilting disk that is displaced proximally towards the ectoplacental cone (EPC) and eventually fuses with the ventral surface of the developing placenta. In *Smad1* mutants, this process is abnormal. While the amniotic folds form and the extra-embryonic mesoderm migrates to the line the VE, the chorion is erratically folded within the exocoelomic cavity (Fig. 2J). Despite the incorrect placement and folding of the chorion at this stage, the composition of this tissue is histologically normal and the chorionic ectoderm is lined with mesoderm (Fig. 2K).

The allantois emerges as a bud of extra-embryonic mesoderm that is continuous with the most posterior aspect of the primitive streak. As the bud expands and projects into the exocoelomic cavity, the proximal portion enlarges via mitosis and cavitation to produce a loosely scattered mesothelium capable of chorioallantoic fusion (Downs, 2000; Ellington, 1985), while the distal cells at the base of the allantois remain densely packed and continuous with the streak. In comparison with wild-type littermates at 7.5-8.5 dpc, the allantois of *Smad1*-mutant embryos fails to elaborate and remains as a compact mass of extra-embryonic mesoderm continuous with the streak (Fig. 2F-M). Unlike the twisting of the mutant epiblast, the growth of the allantois never recovers and thus by 9.5 dpc, three types of allantois-like structures have developed (Fig. 3). The mutant allantois can develop into a balloon-like structure containing peripheral blood-filled vessels (Fig. 3A) or a dense structure filled with compact mesenchyme and small blood-filled sacs (Fig. 3B). In a fraction of the mutants, the allantoic rudiment occasionally forms a tenuous connection

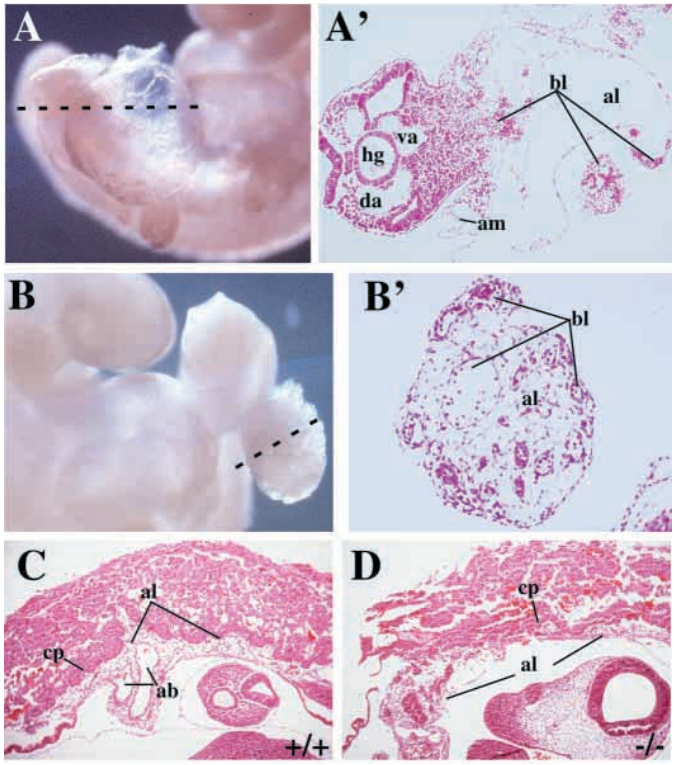

Fig. 3. *Smad1*$^{-/-}$ allantois morphogenesis is abnormal. Three allantois phenotypes are observed in *Smad1*-deficient embryos at 9.5 dpc. The broken line in A,B represents the plane of section in (A′,B′). (A,A′) Some embryos develop a balloon-like structure containing pooled blood. (B,B′) In other mutant embryos, the allantoic rudiment is compact and forms a dense mesenchyme with blood apparent throughout the structure. Frontal sections of wild-type (C) and mutant (D) embryos. (C) The wild-type allantois has prominent blood vessels and has fused uniformly across the entire surface of the chorionic plate. (D) In a proportion of *Smad1*-deficient embryos, the allantois fuses peripherally and non-uniformly.
ab, allantois blood vessel; al, allantois; am, amnion; bl, blood; cp, chorionic plate; da, dorsal aorta; hg, hindgut diverticulum; va, vitelline artery.

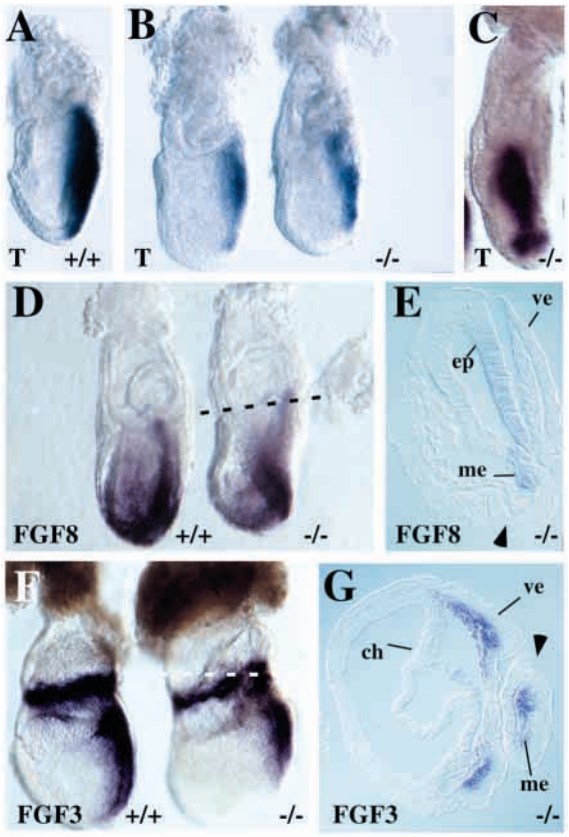

Fig. 4. Disturbed mesoderm formation and migration in *Smad1* mutants. Whole-mount in-situ hybridization of wild-type (+/+) and mutant (–/–) embryos. (A) *T* is normally expressed in the primitive streak and in nascent mesoderm of 7.0 dpc wild-type embryos. (B) In *Smad1*$^{-/-}$ littermates, *T* expression is patchy and less intense. (C) A posterior view of a *Smad1* mutant embryo showing discontinuous *T* expression. (D) *Fgf8*, normally expressed in the nascent mesoderm, streak and at the base of the allantois at 7.0 dpc (left), is similarly expressed in mutant embryos (right), but is distorted, owing to the twisted epiblast. (E) Transverse section of the mutant embryo in D, showing *Fgf8*-expressing cells within the posterior folds (arrowhead). (F) *Fgf3*, expressed in the extra-embryonic mesoderm and streak in wild-type embryos is also present throughout the extra-embryonic folds of mutant embryos. (G) A transverse section of the mutant in F. Anterior is towards the left in all panels except C.
ch, chorion; ep, epiblast; ve, visceral endoderm.

with the chorionic surface of the placenta, but fails to efficiently invade (Fig. 3D).

Other defects observed in a subset of *Smad1*-deficient embryos at 9.5-10.0 dpc include a distended pericardium, delays in ventral closure and incomplete embryonic turning (data not shown). Some of these defects, in particular incomplete turning, may be secondary as the embryos are not tethered to the placenta. Furthermore, *Smad1*-deficient embryos are often irregularly positioned within the yolk-sac and are smaller than their wild-type counterparts, most probably reflecting a nutritive defect resulting from failure to establish a maternal connection.

Molecular characterization of tissue defects

To more carefully analyze the tissue defects in *Smad1* mutant embryos, we used a panel of molecular markers. To establish whether the defects observed in early mesodermal populations originate from defects in the morphogenesis of the primitive streak, *Brachyury* (*T*) expression was assessed. In wild-type embryos, *T* marks the entire PD axis of the streak and nascent mesoderm (Wilkinson et al., 1990; Fig. 4A). By contrast, *Smad1* mutants exhibited discontinuous and less intense *T* expression (Fig. 4B,C). *Fgf8*, a marker of the primitive streak and the base of the allantois, was also examined (Crossley and Martin, 1995). Although expression levels in the streak were comparable with those in wild-type littermates, posterior views of 7.0 dpc mutants demonstrates that the streak is irregularly twisted (Fig. 4D). In many mutants, we noted that the proximal-most domain of *Fgf8* expression lay within the VE folds, presumably demarcating the base of the allantois (Fig. 4D,E). To confirm this possibility, we assessed *Fgf3* expression, a marker for extra-embryonic mesoderm (Wilkinson et al., 1988). As with *Fgf8*, cells within the VE folds express *Fgf3* confirming that extra-embryonic mesoderm migrates into the pockets of VE (Fig. 4F,G).

Reciprocal interactions between the VE and underlying

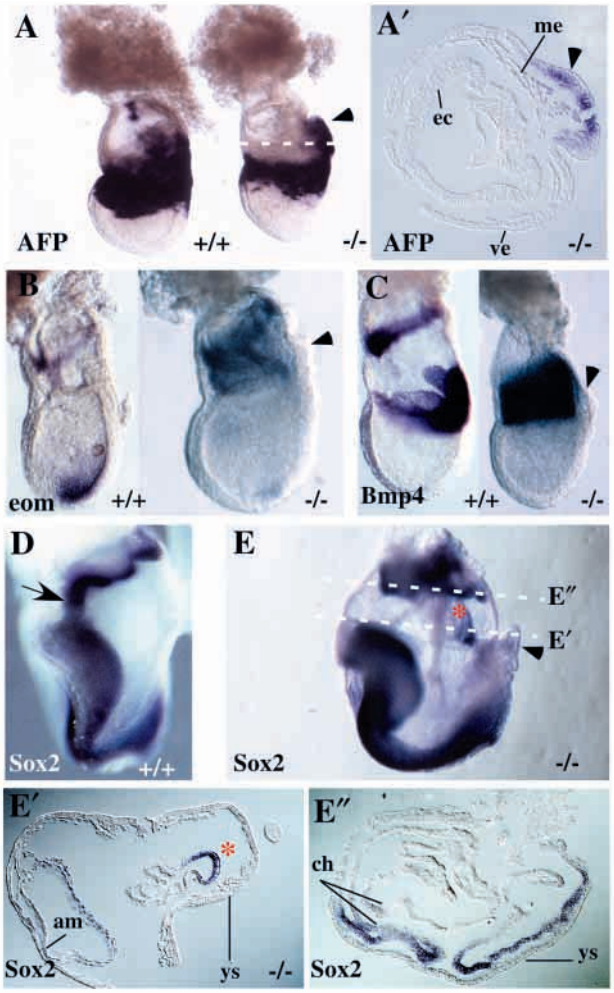

Fig. 5. Extra-embryonic defects in *Smad1*$^{-/-}$ embryos. (A) *Afp* expression in wild-type (left) and mutant (right) 7.5 dpc embryos. Compared with the wild-type littermate, *Afp* is excluded from the anterior extra-embryonic region of the mutant embryo. (A′) A transverse section through the proximal portion of the mutant embryo demonstrates that *Afp* expression is localized to the ruffled VE (arrowhead). (B) *Eomesodermin* (*eom*) expression demarcates the extra-embryonic ectoderm and anterior streak. In *Smad1*$^{-/-}$ embryos, *eom*-positive cells in the extra-embryonic region are greatly expanded. (C) *BMP4* expression delineates the extra-embryonic ectoderm and mesoderm. In the mutant embryo, *BMP4* expression is expanded throughout the extra-embryonic part of the embryo. (D) *Sox2* is expressed throughout the embryonic and extra-embryonic ectoderm of 8.0 dpc embryos. Note the canal of tissue that normally extends from the anterior portion of the chorion towards the head of the embryo (arrow). (E) In 8.0 dpc *Smad1*$^{-/-}$ embryos, *Sox2*-positive tissue emanates from the posterior portion of the embryo towards the chorion (*). (E′) A transverse section through the embryo in (E) demonstrates that the posterior *Sox2* projection (*) is a ring of cells. (E″) A section near the EPC shows the erratic folding of the chorion. am, amnion; ec, ectoderm; me, mesoderm; ve, visceral endoderm; ys, yolk sac.

tissues define gene expression profiles and thus the identity of both tissues. *Alpha foetoprotein* (*AFP*) is initially expressed throughout the VE overlying the embryonic region, but is excluded from the extra-embryonic region, owing to an inhibitory influence from the extra-embryonic ectoderm (Dziadek and Adamson, 1978). Thus, the proximal edge of *AFP* expression normally coincides with the distal edge of the extra-embryonic ectoderm (Fig. 5A). In *Smad1*-mutant embryos, *AFP* expression is normal in the VE overlying the embryonic region. However, *AFP* expression is absent in anterior aspects of the extra-embryonic region (Fig. 5A). Failure to activate *AFP* indicates either an intrinsic defect within the anterior VE or, more likely, that *AFP* induction is repressed by the presence of ectopic extra-embryonic ectoderm (Fig. 5A′).

To distinguish between these possibilities, the expression of two extra-embryonic ectodermal markers, *eomesodermin* (*eom*) and *Bmp4* were examined. At early headfold stages, *eom* expression is detected throughout the ectoderm of the proximally migrating chorionic disk and the anterior streak (Ciruna and Rossant, 1999; Hancock et al., 1999) (Fig. 5B). Similarly, *Bmp4* is expressed in the ectodermal layer of the chorion, as well as in the extra-embryonic mesodermal derivatives (Lawson et al., 1999) (Fig. 5C). In early headfold mutant embryos, both markers are observed throughout the extra-embryonic region, but are excluded from the region occupied by and immediately adjacent to the VE folds (Fig. 5B,C). These results support the hypothesis that the exclusion of *AFP* expression from the VE overlying the extra-embryonic regions of mutant embryos reflects the abnormal migration and/or overproliferation of the extra-embryonic ectoderm.

To determine the extent of embryonic lineage formation as well as the fate of extra-embryonic ectoderm at later stages, we examined *Sox2* expression in late headfold embryos. *Sox2* is normally expressed in the neuroectoderm, definitive endoderm and throughout the extra-embryonic ectoderm (Wood and Episkopou, 1999). In *Smad1* mutants, while the embryonic expression pattern is normal, the extra-embryonic expression pattern is highly aberrant. Unlike wild-type embryos, a *Sox2*-positive projection extends from the posterior proximal edge of the embryonic region towards the EPC (Fig. 5D,E,E′). Proximal sections of *Sox2*-labeled embryos also reveals the presence of a copious amount of erratically folded chorionic ectoderm (Fig. 5E″). Collectively, our analyses show that loss of *Smad1* severely perturbs the growth and morphogenesis of the chorion.

Expression patterns of *Smad1*, *Smad5* and *Smad8*

BMP signals can be transmitted by Smad1, Smad5 and Smad8 (Chen et al., 1997; Hoodless et al., 1996; Kawai et al., 2000; Macias-Silva et al., 1998). To establish any correlation between tissue abnormalities seen in *Smad1* mutants and the pattern of expression of BMP-transducing Smads, we compared the expression pattern of all three genes from early stages onwards. At 6.5 dpc *Smad1* is highly expressed in the VE, and at much lower levels in the early epiblast (Fig. 6A). After the initiation of gastrulation, *Smad1* is expressed at high levels throughout the embryonic and extra-embryonic mesoderm and VE, with lower levels detected in epiblast tissue and chorion (Fig. 6B). By comparison, *Smad5* is expressed at low levels throughout the pre-gastrulation embryos but is markedly upregulated by 7.25 dpc in the entire embryonic and extra-embryonic mesoderm and epiblast (Fig. 6D-E; Chang et al., 1999). *Smad8* is not expressed above background levels at 6.5 dpc (Fig. 6G). By 7.25 dpc, *Smad8* is expressed at the highest levels in the VE, amnion and allantois with lower levels apparent in the posterior streak and chorion (Fig. 6H). Thus, all three BMP-

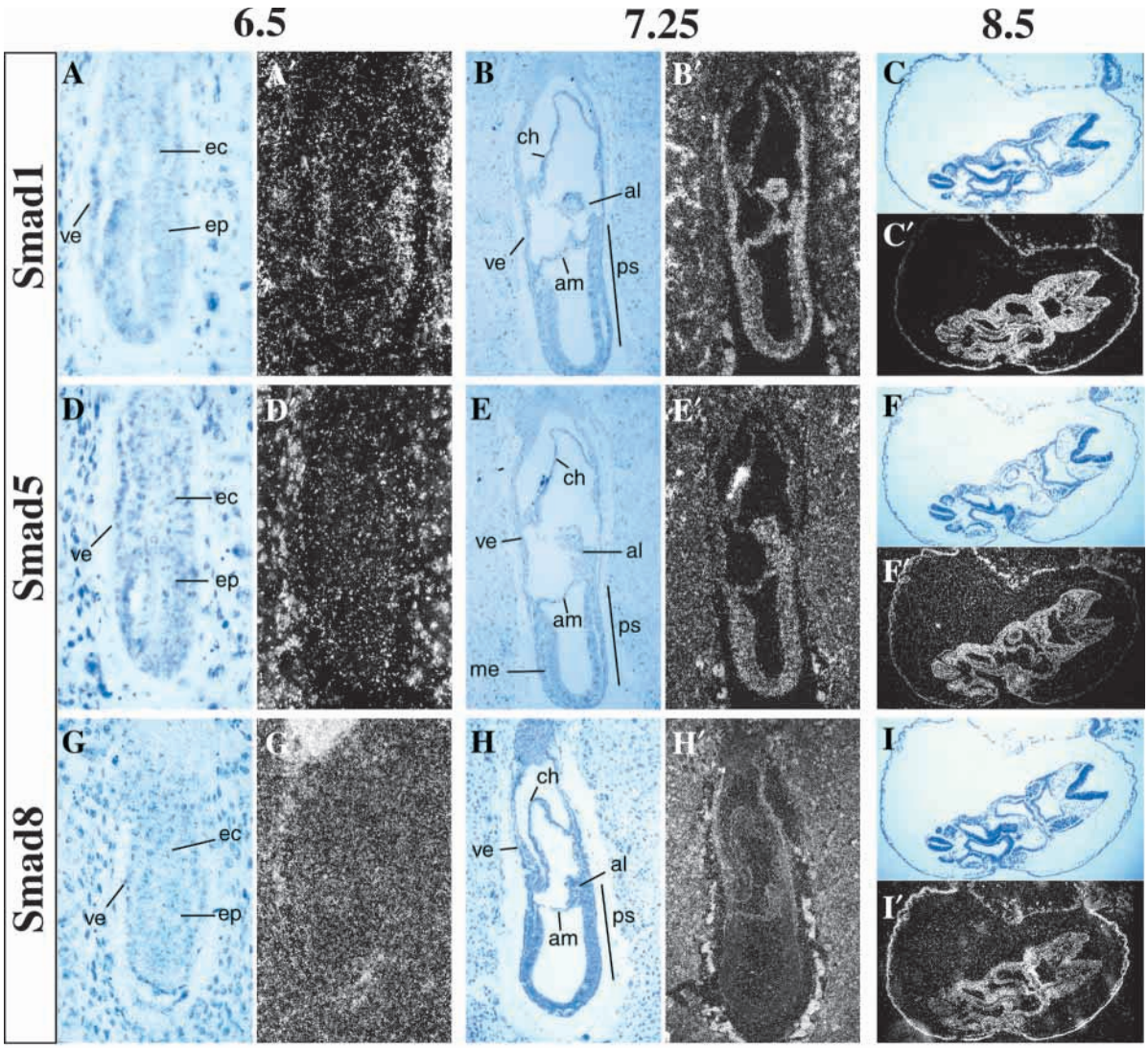

Fig. 6. Expression patterns of *Smad1*, *Smad5* and *Smad8*. Brightfield and darkfield images of sagittally sectioned embryos at 6.5 (A,D,G), 7.25 (B,E,H) and 8.5 dpc (C,F,I) hybridized using *Smad1* (A-C), *Smad5* (D-F) or *Smad8* (G-I) specific probes. (A,A′) At the onset of gastrulation, *Smad1* is highly expressed in the VE and early primitive streak. (B,B′) At late streak stage, *Smad1* is observed in the VE, extra-embryonic and embryonic mesoderm derivatives. as well as the primitive streak. (C,C′) By 8.5 dpc, *Smad1* is ubiquitously expressed. (D,D′) At 6.5 dpc *Smad5* is uniformly expressed at low levels throughout the conceptus. (E,E′) At late streak stages, *Smad5* is expressed throughout the embryonic region and the allantois. (F,F′) *Smad5* transcripts are found throughout 8.5 dpc embryos. (G,G′) At 6.5 dpc a *Smad8* hybridization signal cannot be discerned from background. (H,H′) At late primitive streak stages, *Smad8* is expressed in the VE, posterior primitive streak and extra-embryonic mesoderm derivatives. (I,I′) By 8.5 dpc *Smad8* is widely expressed. al, allantois; am, amnion; ch, chorion; ec, ectoderm; ep, epiblast; ps, primitive streak; ve, visceral endoderm.

transducing Smads are co-expressed in the extra-embryonic mesoderm populations at 7.25 dpc, while only *Smad1* and *Smad8* are abundantly expressed in the VE. By 8.5 dpc, all three genes are uniformly and ubiquitously expressed in the embryo (Fig. 6C,F,I). These results demonstrate that while *Smad1* is uniquely expressed in the early VE, by the onset of gastrulation all tissues express multiple BMP-transducing Smads.

Autonomy of the VE defect

Embryonic stem (ES) cells introduced into blastocysts predominantly colonize the epiblast (Beddington and Robertson, 1989). Thus, in chimeric embryos, ES cell derivatives are confined to the embryo, while the extra-embryonic lineages are colonized exclusively by the host blastocyst. This developmental bias has routinely been used to discern the role of specific molecules in the epiblast versus extra-embryonic tissues. We therefore generated chimeric embryos to determine if the defects observed in *Smad1*-deficient embryos are due solely to the requirement for Smad1 in the VE and extra-embryonic ectoderm or reflect a requirement for Smad1-mediated BMP signaling in the epiblast and its derivatives. *lacZ*-marked wild-type cells (Tremblay et al., 2000) were injected into blastocysts derived from $Smad1^{Robm1}$ heterozygous intercrosses. In this experiment, 25% of the chimeras are expected to be composed of *Smad1*-deficient primitive endoderm and extra-embryonic ectoderm. Chimeric embryos were recovered for analysis at 7.5

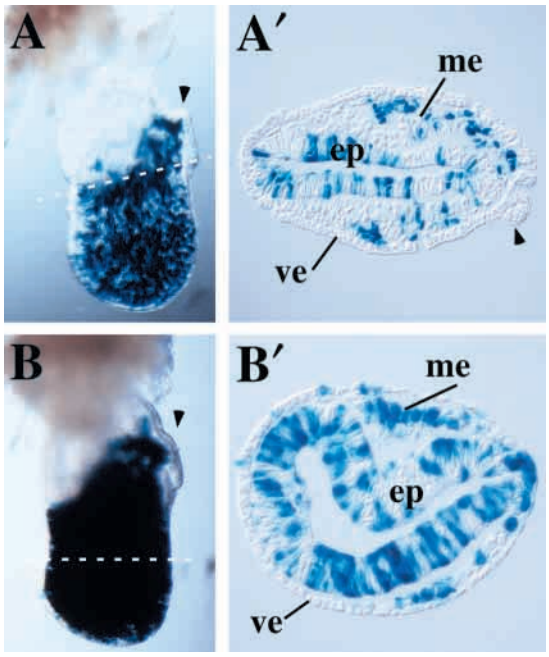

Fig. 7. Colonization of *Smad1* mutant embryos by wild-type ES cells fails to rescue gastrulation defects. Chimeras were generated by injecting *lacZ*-positive wild-type ES cells into host blastocysts collected from *Smad1*$^{+/-}$ intercrosses. (A,B) Two examples of *Smad1*$^{-/-}$ embryos significantly colonized by wild-type ES cells. (A,A′) The posterior visceral endoderm defect is apparent in whole-mount and transverse section. (B,B′) A distal section from a second strongly chimeric embryo illustrates that the twisting of the epiblast is not rescued by the presence of wild-type cells. The arrowhead points to the VE ruffles. Anterior is towards the left in all panels. ep, epiblast; me, mesoderm; ve, visceral endoderm.

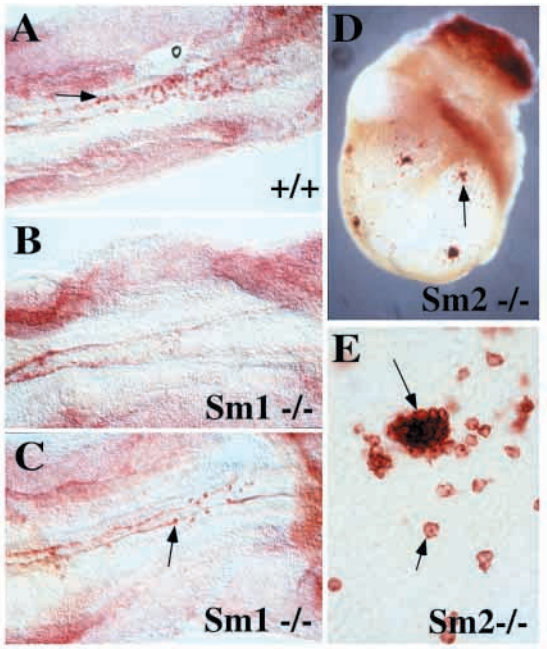

Fig. 8. Reduced numbers of PGCs in *Smad1*, but not *Smad2*, mutant embryos. (A-C) Dorsal views of alkaline phosphatase (AP)-stained, wild-type and *Smad1* mutant hindgut pieces at the 17 somite stage. Arrows indicate PGCs. (A) Wild-type embryo with 87 PGCs. Smad1 homozygous mutants with (B) no PGCs or (C) 14 PGCs. (D) Abundant AP-positive PGCs in an advanced *Smad2*$^{-/-}$ embryo are mostly present in foci. (E) High-power magnification of a PGC cluster showing that the darkly staining foci contain typical PGCs with a characteristic cytoplasmic spot and darkly staining cell membrane.

dpc. Six out of 28 (21%) displayed both a ruffled posterior visceral endoderm and a twisted epiblast phenotype (Fig. 7A,B). Of these, three were colonized predominately by *lacZ*-positive derivatives. This result suggests that the VE defect and the distortion of the egg cylinder can be attributed to the lack of *Smad1* in the extra-embryonic lineages.

Smad1 and primordial germ cell formation

Cell lineage analysis has shown that at 6.0 dpc the precursors of the primordial germ cells (PGCs) lie in the extreme proximal epiblast adjacent to the extra-embryonic ectoderm (Lawson and Hage, 1994). This precursor population gives rise to descendants not only in the germline, but also in the extra-embryonic mesoderm, including allantois. Recent genetic and embryological experiments show that BMP signals emanating from the extra-embryonic ectoderm act directly on the proximal epiblast, and are required for the formation of PGCs and allantois (Lawson and Hage, 1994; Ying et al., 2000; Yoshimizu et al., 2001). Because of the biochemical evidence that places Smad1 downstream of BMP signals and because of the abnormal allantois morphogenesis in *Smad1* null mutants, we chose to investigate the potential involvement of Smad1 in PGC development.

Allocation to the germ cell lineage is thought to occur shortly before PGCs can first be identified as a cluster of strongly alkaline phosphatase (AP)-positive cells at the base of the allantois (Ginsburg et al., 1990; Lawson and Hage, 1994). Around 8.5 dpc, the PGCs intercalate into the hindgut epithelium and migrate anteriorly. We collected *Smad1*-deficient embryos at 9.0-9.5 dpc and assayed for PGC formation by staining for endogenous AP activity. While wild-type and heterozygous littermates between 13 and 26 somites all had similar numbers of PGCs (n=80-250), the number observed in mutant embryos was significantly reduced (Fig. 8A-C). Of the 14 similarly staged mutants, six out of 14 (43%) had no PGCs, five out of 14 (36%) had fewer than ten and three out of 14 (21%) had less than 25. These results suggest that loss of *Smad1* affects either the initial specification of the PGC precursor population in the proximal epiblast or survival and/or proliferation of the allocated PGC population. Further support for the role of Smad1 in the early specification of PGCs comes from the analysis of PGC numbers at the late headfold (LHF)-stage, when early PGCs are visible as a cluster at the base of the allantois. Consistent with the deficit of PGCs in later embryos, HF-stage *Smad1*$^{-/-}$ either lack or contain less than three PGCs (data not shown). An alternative explanation is that the severe posterior streak defects in *Smad1*-null embryos compromise local signals within the extra-embryonic lineages that may play a role in the allocation of the PGC precursors to the germline or affect their immediate survival. To control for this possibility, we examined PGC formation in *Smad2*-deficient embryos. *Smad2* mutants embryos do not form a recognizable primitive streak, and by 8.0 dpc the entire epiblast

transforms into extra-embryonic mesoderm (Waldrip et al., 1998). In spite of these profound cellular disturbances, we found that the majority of Smad2-deficient embryos (20/25) collected at 8.5 dpc contained PGCs. Several *Smad2* mutants formed abundant PGCs, many of which were concentrated in darkly stained clusters (Fig. 8D,E). The remaining *Smad2* mutants (5/25) exhibited a more severe phenotype, and completely lacked AP-positive cells (data not shown). Collectively, these data suggest that the formation of PGCs from the proximal epiblast can proceed even in the absence of normal gastrulation movements. Therefore, as opposed to a secondary consequence of aberrant gastrulation, the deficit of PGCs in *Smad1* mutant embryos most probably reflects a direct requirement for Smad1 in transducing extra-embryonic ectoderm-derived BMP signals

DISCUSSION

Members of the TGFβ superfamily of extracellular signaling molecules and their cognate receptors play a variety of roles during vertebrate embryogenesis. We show that Smad1, a downstream component of the BMP signaling pathway, is essential for coordinating the growth and elaboration of extra-embryonic tissues of the mouse embryo (Goumans and Mummery, 2000). This finding is consistent with the observation that multiple BMP ligands are expressed in both embryonic and extra-embryonic tissues from postimplantation stages onwards.

Smad1-mutant embryos are readily identified as early as 7.0 dpc, owing to the localized overgrowth of the VE adjacent to the posterior embryonic/extra-embryonic boundary. Despite the localized tissue disturbance, *Smad1* transcripts are uniformly expressed throughout the VE (Fig. 6A-C). Intriguingly, *Bmp2* is asymmetrically expressed at the onset of gastrulation (Ying and Zhao, 2001), with the highest levels in the VE overlying the proximal regions of the primitive streak. However, the VE defects seen in *Smad1*$^{-/-}$ embryos cannot be attributed to the attenuation of BMP2 signaling alone, because embryos lacking BMP2 do not exhibit this phenotype (Zhang and Bradley, 1996). *Bmp4* and *Bmp8b* are expressed in tissues adjacent to the affected VE population, but neither molecule nor other components of the BMP signaling pathway are known to be asymmetrically distributed. In contrast *cerberus-like* (*Cer1*), an antagonist of both BMP and Nodal signaling (Piccolo et al., 1999) is confined to the VE overlying the anterior side of the embryo. While *Cer1* is not essential for development (Belo et al., 2000; Shawlot et al., 2000; Simpson et al., 1999), the anterior expression of *Cer1* as well as that of other antagonists, such as *dickkopf1*and *lefty1* (Glinka et al., 1998; Meno et al., 1999), suggests a mechanism that limits the levels of activated Smad1 anteriorly. Given the expression patterns of the antagonists and the BMP ligands during early gastrulation, it is likely that the uniform expression of *Smad1* in the VE is converted to a posterior activity gradient. Our data is consistent with this Smad1 activity playing an important role in negatively regulating posterior VE growth.

The overgrowth of the VE in *Smad1*-deficient embryos is causally associated with a pronounced twisting of the epiblast and mesoderm tissue along the PD axis. Thus, we find that neither defect is rescued in chimeric embryos in which the epiblast derivatives are largely wild type, suggesting that this phenotype results from the lack of Smad1 in extra-embryonic tissues, most likely the VE where *Smad1* is highly expressed (Fig. 6A-C). Remarkably, the morphogenetic disturbances are relatively transient, as judged by whole-mount, histological and molecular criteria, and all mutant embryos regain bilateral symmetry by 8.0 dpc. Interestingly the correction of the phenotype is coincident with formation of the definitive endoderm, the cell population that displaces the VE. Thus, one likely explanation for the recovery of bilateral symmetry is that the replacement of the VE by the emerging definitive endoderm, which is specified normally in *Smad1*$^{-/-}$ embryos, relieves the mechanical restrictions imposed by the VE. Interestingly, loss of function of other transcription factors expressed in the VE result in altered epiblast morphology (Acampora et al., 1995; Ang et al., 1996; Ang and Rossant, 1994; Shawlot and Behringer, 1995). In these cases, abnormal morphogenesis of VE causes a constriction at the embryonic/extra-embryonic boundary. Chimera analysis confirms that these defects reside in the extra-embryonic tissues, further supporting the idea that defects in the VE secondarily impact epiblast morphogenesis (Dufort et al., 1998; Rhinn et al., 1998; Shawlot et al., 1999). Importantly, unlike *Smad1* mutants, these mutations are more severe and disturb the formation of the primary embryonic axis and are often associated with defects in the definitive endoderm.

In *Smad1* mutants, *T* expression is severely perturbed during early/mid-streak stages, but is present at normal levels by 7.5-8.0 dpc (Fig. 4A-C; data not shown). *T* is normally uniformly expressed in nascent mesoderm forming along the entire length of the primitive streak. However in the absence of Smad1, we find reduced and intermittent *T* expression. Strikingly, at these early stages, other streak and mesoderm markers, including *Fgf8*, *Fgf3* and *eom* are also expressed in an irregular pattern, indicative of the disrupted PD axis noted above, but in contrast to *T*, these markers are expressed at wild-type levels (Fig. 4D; data not shown). One possibility for the selective reduction of *T* expression is that Smad1 is involved in the activation of early *T* expression. Indeed, in *T* mutants and *T* chimeras allantois formation is impaired, and resembles what we describe here for *Smad1*-deficient embryos (Rashbass et al., 1991; Wilson et al., 1993). A recent report has suggested that SIP1, a novel zinc-finger/homeodomain protein, can interact with both activated Smads and target gene promoters. Interestingly, SIP1 binding motifs have been identified in the Xenopus *T* homolog (Verschueren et al., 1999), providing evidence in support of a Smad1-mediated pathway regulating *T* transcription.

Previous gene targeting experiments have underscored the importance of BMP signaling in the formation of the allantois. Embryos that lack *Bmp4* form a rudimentary allantois (Lawson et al., 1999), while in *Bmp2* mutants, allantois formation is slightly delayed (Zhang and Bradley, 1996). Embryos that lack *Bmp8b*, a member of the 60A subgroup of BMP ligands, have a shortened allantois attributed to developmental delay (Ying et al., 2000). Other members of the 60A subgroup are not uniquely important for allantois formation, but in *Bmp5*/7 double mutant embryos the allantois is reduced in size, developmentally delayed and often unable to fuse with the chorion (Solloway and Robertson, 1999). Interestingly, despite the robust co-expression of *Smad1*, *Smad5* and *Smad8* in the allantois (Fig. 6) and adjacent tissues,

loss of either *Smad1* or *Smad5* results in distinct allantois phenotypes. *Smad5*-deficient embryos show a marked delay in allantois development, and in severely affected mutants the allantois fails to fuse with the chorion and may become displaced onto the amnion (Chang et al., 1999; Yang et al., 1999a). Loss of Smad1 has a more pronounced impact on allantois formation. Thus, at 8.0 dpc, while control littermates have produced an extended allantois composed of differentiated cell populations (Fig. 2H,L,M) in *Smad1*-deficient embryos the allantois forms a compact mass of cells that is continuous with the primitive streak (Fig. 2F,G,I-K). By 9.5 dpc, the *Smad1*$^{-/-}$ allantois develops into an unpatterned mass of tissue containing vascular endothelium and red blood cells (Fig. 3). Taken together, these results suggest that although allantois-like tissue is specified during gastrulation, the allantois rudiment that forms in *Smad1* mutants is defective in proliferation and patterning. These results are provocative because neither the *Smad1* or the *Smad5* loss-of-function mutation fully recapitulate the allantois phenotype of any one BMP mutant, suggesting that a single BMP activates multiple Smads. Furthermore, these distinct phenotypes suggest that Smad1 and Smad5 play discrete roles in the development of the allantois; Smad5 signals govern the timing of development and migration, while Smad1 signals direct proliferation and patterning.

Elegant cell marking experiments have demonstrated that the progenitors of the allantois and the primordial germ cells are located in the proximal region of the epiblast, close to the embryonic/extra-embryonic junction (Lawson and Hage, 1994). BMP4 and BMP8b, synthesized in the extra-embryonic ectoderm, are required for the generation of this precursor population (Lawson et al., 1999; Ying et al., 2000), and recent embryological experiments suggest that the BMP ligands act directly on the epiblast (Lawson et al., 1999). Consistent with these findings, we show that *Smad1* is expressed at low levels within the epiblast (Fig. 6A), and that *Smad1* mutants have drastically reduced numbers of PGCs. The simplest explanation for the marked impact on PGC formation in *Smad1* mutants is that cells of the proximal epiblast are severely impaired in their ability to transduce extra-embryonic ectoderm produced BMP4/BMP8b signals. Consequently, very few to no cells are specified as PGC precursors. Furthermore, the presence of PGCs in about 50% of *Smad1* mutants suggests that the requirement for Smad1 is not absolute, and that Smad5, which is also expressed at low levels in the epiblast, may partially compensate for the absence of Smad1 in some cells. Whether loss of Smad5 also impairs PGC development has yet to be reported.

A two-step model for the production of PGCs has been proposed, based on the estimation that allocation to the germ cell lineage occurs around 7.2 dpc, after the precursor population emerges from the posterior primitive streak in the nascent extra-embryonic mesoderm (Lawson et al., 1999). In this model, BMP4/BMP8b produced by the extra-embryonic ectoderm specifies a population of PGC and allantois progenitor cells in the proximal epiblast. A second signal originating in or adjacent to the proximal streak then instructs these precursor cells into either an allantois or PGC lineage. The abundant expression of *Smad1* in the posterior streak, extra-embryonic mesoderm and VE, suggests that Smad1 may be a component of this putative 'second signal', responding to locally high levels of BMP2 produced by the posterior VE, or BMP4 synthesized in the newly formed extra-embryonic mesoderm. To refine our understanding of the tissue-specific requirements for Smad1 that underlie these events, a future goal will be to exploit the conditional allele to selectively remove Smad1 from different tissue compartments of the early embryo.

A unique aspect of the *Smad1* phenotype, not shared by other mutations in BMP pathway genes, is our finding that Smad1 is required for growth and morphogenesis of the chorion. The chorion, composed of both extra-embryonic ectoderm and mesoderm, is an essential component of the mature placenta. Coincident with gastrulation, the extra-embryonic ectoderm and an accompanying layer of extra-embryonic mesoderm, move proximally towards the EPC. This proximal movement and regulated growth appears to be an intrinsic property of the chorion, as in embryos that lack most epiblast derivatives or are defective in allantois morphogenesis, chorion development proceeds normally (Chang et al., 1999; Gurtner et al., 1995; Kwee et al., 1995; Waldrip et al., 1998; Yang et al., 1995; Yang et al., 1999a). Thus, the chorion defects observed in *Smad1* mutant embryos are likely to be due to a requirement for Smad1 activity in this tissue. Interestingly, as is the case with the posterior VE, the chorion represents a second site in the embryo where loss of Smad1 results in massive overgrowth of cells, implicating Smad1 pathways in regulating the growth of these specific tissues. Because *Smad1* is expressed in both the mesodermal and ectodermal components of the chorion, it remains to be determined whether Smad1 signals in the extra-embryonic ectoderm regulate the growth of the extra-embryonic mesoderm or vice versa.

In addition to appropriate specification and differentiation of distinct cell types, the coordinated growth and morphogenesis of various tissue layers is also an important feature of the developing embryo. BMP signaling pathways have been shown to participate in controlling the growth of the embryo. In the present study, we have uncovered a role for Smad1 in regulating the formation and proliferation of the chorion, allantois and VE, as well as PGCs. Interestingly, Smad1 acts to inhibit growth of the chorion and VE, while Smad1 activities promote growth of the allantois and formation of PGCs. Recent reports demonstrate the widespread expression of Smad1 during later embryogenesis (Dick et al., 1998; Huang et al., 2000) and BMP signaling pathways make important contributions to developing organ systems such as the eyes, lungs and kidneys (Bellusci et al., 1996; Dudley et al., 1999; Dudley et al., 1995; Weaver et al., 1999). Future experiments should aim to explore the unique contribution of Smad1 to these later processes, using the conditional allele to bypass the early extra-embryonic defects.

Note added in proof

A defect in primorial germ cell development was recently reported by Chang and Matzuk (Chang, H. and Matzuk, M. M. (2001). *Smad5* is required for mouse primordial germ cell development. *Mech. Dev.* **104**, 61-67).

We thank Pamela Hoodless and Jeff Wrana for the Smad1 cDNA and hSmad1 expression vector, Liz Bikoff, Ross Waldrip and Audrey Jackson for isolation and initial characterization of genomic clones,

Juliana Brown for assistance with the Robm1 construct, Gerry Chu for the Smad8 probe, Debbie Pelusi for assistance with genotyping, Jane Brennan, Rob Godin and Matt Deardorff for comments on the manuscript, and Patti Lewko and Joe Rocca for expert animal care. K. D. T. and N. R. D. were supported by postdoctoral fellowship grants from the NICHD. This work was supported by a grant from the NIH to E. J. R.

REFERENCES

Acampora, D., Mazan, S., Lallemand, Y., Avantaggiato, V., Maury, M., Simeone, A. and Brulet, P. (1995). Forebrain and midbrain regions are deleted in Otx2$^{-/-}$ mutants due to a defective anterior neuroectoderm specification during gastrulation. *Development* **121**, 3279-3290.

Ang, S. L. and Rossant, J. (1994). HNF-3 beta is essential for node and notochord formation in mouse development. *Cell* **78**, 5615-74.

Ang, S. L., Jin, O., Rhinn, M., Daigle, N., Stevenson, L. and Rossant, J. (1996). A targeted mouse Otx2 mutation leads to severe defects in gastrulation and formation of axial mesoderm and to deletion of rostral brain. *Development* **122**, 243-252.

Baker, J. C. and Harland, R. M. (1996). A novel mesoderm inducer, Madr2, functions in the activin signal transduction pathway. *Genes Dev.* **10**, 1880-1889.

Beddington, R. S. and Robertson, E. J. (1989). An assessment of the developmental potential of embryonic stem cells in the midgestation mouse embryo. *Development* **105**, 733-737.

Beddington, R. S. and Robertson, E. J. (1999). Axis development and early asymmetry in mammals. *Cell* **96**, 195-209.

Bellusci, S., Henderson, R., Winnier, G., Oikawa, T. and Hogan, B. L. (1996). Evidence from normal expression and targeted misexpression that bone morphogenetic protein (Bmp-4) plays a role in mouse embryonic lung morphogenesis. *Development* **122**, 1693-1702.

Belo, J. A., Bachiller, D., Agius, E., Kemp, C., Borges, A. C., Marques, S., Piccolo, S. and De Robertis, E. M. (2000). Cerberus-like is a secreted BMP and nodal antagonist not essential for mouse development. *Genesis* **26**, 265-270.

Chang, H., Huylebroeck, D., Verschueren, K., Guo, Q., Matzuk, M. M. and Zwijsen, A. (1999). Smad5 knockout mice die at mid-gestation due to multiple embryonic and extraembryonic defects. *Development* **126**, 1631-1642.

Chang, H., Zwijsen, A., Vogel, H., Huylebroeck, D. and Matzuk, M. M. (2000). Smad5 is essential for left-right asymmetry in mice. *Dev. Biol.* **219**, 71-78.

Chen, Y., Bhushan, A. and Vale, W. (1997). Smad8 mediates the signaling of the ALK-2 receptor serine kinase. *Proc. Natl. Acad. Sci. USA* **94**, 12938-12943.

Ciruna, B. G. and Rossant, J. (1999). Expression of the T-box gene Eomesodermin during early mouse development. *Mech. Dev.* **81**, 199-203.

Conlon, F. L., Lyons, K. M., Takaesu, N., Barth, K. S., Kispert, A., Herrmann, B. and Robertson, E. J. (1994). A primary requirement for nodal in the formation and maintenance of the primitive streak in the mouse. *Development* **120**, 1919-1928.

Crossley, P. H. and Martin, G. R. (1995). The mouse Fgf8 gene encodes a family of polypeptides and is expressed in regions that direct outgrowth and patterning in the developing embryo. *Development* **121**, 439-451.

Dick, A., Risau, W. and Drexler, H. (1998). Expression of Smad1 and Smad2 during embryogenesis suggests a role in organ development. *Dev. Dyn.* **211**, 293-305.

Downs, K. M. (2000). Growth in the pre-fusion murine allantois. *Anat. Embryol.* **202**, 323-331.

Dudley, A. T., Lyons, K. M. and Robertson, E. J. (1995). A requirement for bone morphogenetic protein-7 during development of the mammalian kidney and eye. *Genes Dev.* **9**, 2795-2807.

Dudley, A. T., Godin, R. E. and Robertson, E. J. (1999). Interaction between FGF and BMP signaling pathways regulates development of metanephric mesenchyme. *Genes Dev.* **13**, 1601-1613.

Dufort, D., Schwartz, L., Harpal, K. and Rossant, J. (1998). The transcription factor HNF3beta is required in visceral endoderm for normal primitive streak morphogenesis. *Development* **125**, 3015-3025.

Dziadek, M. and Adamson, E. (1978). Localization and synthesis of alphafoetoprotein in post-implantation mouse embryos. *J. Embryol. Exp. Morphol.* **43**, 289-313.

Ellington, S. K. (1985). A morphological study of the development of the allantois of rat embryos in vivo. *J. Anat.* **142**, 1-11.

Ginsburg, M., Snow, M. H. and McLaren, A. (1990). Primordial germ cells in the mouse embryo during gastrulation. *Development* **110**, 521-528.

Glinka, A., Wu, W., Delius, H., Monaghan, A. P., Blumenstock, C. and Niehrs, C. (1998). Dickkopf-1 is a member of a new family of secreted proteins and functions in head induction. *Nature* **391**, 357-362.

Goumans, M. J. and Mummery, C. (2000). Functional analysis of the TGFbeta receptor/Smad pathway through gene ablation in mice. *Int. J. Dev. Biol.* **44**, 253-265.

Graff, J. M., Bansal, A. and Melton, D. A. (1996). Xenopus Mad proteins transduce distinct subsets of signals for the TGF beta superfamily. *Cell* **85**, 479-487.

Gurtner, G. C., Davis, V., Li, H., McCoy, M. J., Sharpe, A. and Cybulsky, M. I. (1995). Targeted disruption of the murine VCAM1 gene: essential role of VCAM-1 in chorioallantoic fusion and placentation. *Genes Dev.* **9**, 1-14.

Hancock, S. N., Agulnik, S. I., Silver, L. M. and Papaioannou, V. E. (1999). Mapping and expression analysis of the mouse ortholog of Xenopus Eomesodermin. *Mech. Dev.* **81**, 205-208.

Heyer, J., Escalante-Alcalde, D., Lia, M., Boettinger, E., Edelmann, W., Stewart, C. L. and Kucherlapati, R. (1999). Postgastrulation Smad2-deficient embryos show defects in embryo turning and anterior morphogenesis. *Proc. Natl. Acad. Sci. USA* **96**, 12595-12600.

Hoodless, P. A., Haerry, T., Abdollah, S., Stapleton, M., O'Connor, M. B., Attisano, L. and Wrana, J. L. (1996). MADR1, a MAD-related protein that functions in BMP2 signaling pathways. *Cell* **85**, 489-500.

Huang, S., Flanders, K. C. and Roberts, A. B. (2000). Characterization of the mouse smad1 gene and its expression pattern in adult mouse tissues. *Gene* **258**, 43-53.

Jones, C. M., Lyons, K. M. and Hogan, B. L. (1991). Involvement of Bone Morphogenetic Protein-4 (BMP-4) and Vgr-1 in morphogenesis and neurogenesis in the mouse. *Development* **111**, 531-542.

Kawai, S., Faucheu, C., Gallea, S., Spinella-Jaegle, S., Atfi, A., Baron, R. and Roman, S. R. (2000). Mouse smad8 phosphorylation downstream of BMP receptors ALK-2, ALK-3, and ALK-6 induces its association with Smad4 and transcriptional activity. *Biochem. Biophys. Res. Commun.* **271**, 682-687.

Kingsley, D. M. (1994). The TGF-beta superfamily: new members, new receptors, and new genetic tests of function in different organisms. *Genes Dev.* **8**, 133-146.

Kwee, L., Baldwin, H. S., Shen, H. M., Stewart, C. L., Buck, C., Buck, C. A. and Labow, M. A. (1995). Defective development of the embryonic and extraembryonic circulatory systems in vascular cell adhesion molecule (VCAM-1) deficient mice. *Development* **121**, 489-503.

Lawson, K. A. and Hage, W. J. (1994). Clonal analysis of the origin of primordial germ cells in the mouse. *Ciba Found. Symp.* **182**, 68-84.

Lawson, K. A., Meneses, J. J. and Pedersen, R. A. (1991). Clonal analysis of epiblast fate during germ layer formation in the mouse embryo. *Development* **113**, 891-911.

Lawson, K. A., Dunn, N. R., Roelen, B. A., Zeinstra, L. M., Davis, A. M., Wright, C. V., Korving, J. P. and Hogan, B. L. (1999). Bmp4 is required for the generation of primordial germ cells in the mouse embryo. *Genes Dev.* **13**, 424-36.

Luo, J., Sladek, R., Bader, J. A., Matthyssen, A., Rossant, J. and Giguere, V. (1997). Placental abnormalities in mouse embryos lacking the orphan nuclear receptor ERR-beta. *Nature* **388**, 778-782.

Macias-Silva, M., Abdollah, S., Hoodless, P. A., Pirone, R., Attisano, L. and Wrana, J. L. (1996). MADR2 is a substrate of the TGFbeta receptor and its phosphorylation is required for nuclear accumulation and signaling. *Cell* **87**, 1215-1224.

Macias-Silva, M., Hoodless, P. A., Tang, S. J., Buchwald, M. and Wrana, J. L. (1998). Specific activation of Smad1 signaling pathways by the BMP7 type I receptor, ALK2. *J Biol Chem* **273**, 25628-25636.

Massague, J. (1998). TGF-beta signal transduction. *Annu. Rev. Biochem.* **67**, 753-791.

Meersseman, G., Verschueren, K., Nelles, L., Blumenstock, C., Kraft, H., Wuytens, G., Remacle, J., Kozak, C. A., Tylzanowski, P., Niehrs, C. et al. (1997). The C-terminal domain of Mad-like signal transducers is sufficient for biological activity in the Xenopus embryo and transcriptional activation. *Mech. Dev.* **61**, 127-140.

Meno, C., Gritsman, K., Ohishi, S., Ohfuji, Y., Heckscher, E., Mochida, K., Shimono, A., Kondoh, H., Talbot, W. S., Robertson, E. J. et al.

(1999). Mouse Lefty2 and zebrafish antivin are feedback inhibitors of nodal signaling during vertebrate gastrulation. *Mol. Cell* **4**, 287-298.

Nishimura, R., Kato, Y., Chen, D., Harris, S. E., Mundy, G. R. and Yoneda, T. (1998). Smad5 and DPC4 are key molecules in mediating BMP-2-induced osteoblastic differentiation of the pluripotent mesenchymal precursor cell line C2C12. *J. Biol. Chem.* **273**, 1872-1879.

Nomura, M. and Li, E. (1998). Smad2 role in mesoderm formation, left-right patterning and craniofacial development. *Nature* **393**, 786-790.

O'Gorman, S., Dagenais, N. A., Qian, M. and Marchuk, Y. (1997). Protamine-Cre recombinase transgenes efficiently recombine target sequences in the male germ line of mice, but not in embryonic stem cells. *Proc. Natl. Acad. Sci. USA* **94**, 14602-14607.

Piccolo, S., Agius, E., Leyns, L., Bhattacharyya, S., Grunz, H., Bouwmeester, T. and De Robertis, E. M. (1999). The head inducer Cerberus is a multifunctional antagonist of Nodal, BMP and Wnt signals. *Nature* **397**, 707-710.

Rashbass, P., Cooke, L. A., Herrmann, B. G. and Beddington, R. S. P. (1991). A cell autonomous function of Brachyury in T/T embryonic stem cell chimaeras. *Nature* **353**, 348-351.

Rhinn, M., Dierich, A., Shawlot, W., Behringer, R. R., Le Meur, M. and Ang, S. L. (1998). Sequential roles for Otx2 in visceral endoderm and neuroectoderm for forebrain and midbrain induction and specification. *Development* **125**, 845-856.

Robertson, E., Bradley, A., Kuehn, M. and Evans, M. (1986). Germ-line transmission of genes introduced into cultured pluripotential cells by retroviral vector. *Nature* **323**, 445-448.

Russ, A. P., Wattler, S., Colledge, W. H., Aparicio, S. A., Carlton, M. B., Pearce, J. J., Barton, S. C., Surani, M. A., Ryan, K., Nehls, M. C. et al. (2000). Eomesodermin is required for mouse trophoblast development and mesoderm formation. *Nature* **404**, 95-99.

Schier, A. F. and Shen, M. M. (2000). Nodal signaling in vertebrate development. *Nature* **403**, 385-389.

Shawlot, W. and Behringer, R. R. (1995). Requirement for Lim1 in head-organizer function. *Nature* **374**, 425-430.

Shawlot, W., Wakamiya, M., Kwan, K. M., Kania, A., Jessell, T. M. and Behringer, R. R. (1999). Lim1 is required in both primitive streak-derived tissues and visceral endoderm for head formation in the mouse. *Development* **126**, 4925-4932.

Shawlot, W., Min Deng, J., Wakamiya, M. and Behringer, R. R. (2000). The cerberus-related gene, Cerr1, is not essential for mouse head formation. *Genesis* **26**, 253-258.

Simpson, E. H., Johnson, D. K., Hunsicker, P., Suffolk, R., Jordan, S. A. and Jackson, I. J. (1999). The mouse Cer1 (Cerberus related or homologue) gene is not required for anterior pattern formation. *Dev. Biol.* **213**, 202-206.

Solloway, M. J. and Robertson, E. J. (1999). Early embryonic lethality in Bmp5;Bmp7 double mutant mice suggests functional redundancy within the 60A subgroup. *Development* **126**, 1753-1768.

Suzuki, A., Chang, C., Yingling, J. M., Wang, X. F. and Hemmati-Brivanlou, A. (1997). Smad5 induces ventral fates in Xenopus embryo. *Dev. Biol.* **184**, 402-405.

Tremblay, K. D., Hoodless, P. A., Bikoff, E. K. and Robertson, E. J. (2000). Formation of the definitive endoderm in mouse is a Smad2-dependent process. *Development* **127**, 3079-3090.

Verschueren, K., Remacle, J. E., Collart, C., Kraft, H., Baker, B. S., Tylzanowski, P., Nelles, L., Wuytens, G., Su, M. T., Bodmer, R. et al. (1999). SIP1, a novel zinc finger/homeodomain repressor, interacts with Smad proteins and binds to 5′-CACCT sequences in candidate target genes. *J. Biol. Chem.* **274**, 20489-20498.

Waldrip, W. R., Bikoff, E. K., Hoodless, P. A., Wrana, J. L. and Robertson, E. J. (1998). Smad2 signaling in extraembryonic tissues determines anterior-posterior polarity of the early mouse embryo. *Cell* **92**, 797-808.

Weaver, M., Yingling, J. M., Dunn, N. R., Bellusci, S. and Hogan, B. L. M. (1999). Bmp signaling regulates proximal-distal differentiation of endoderm in mouse lung development. *Development* **126**, 4005-4015.

Weinstein, M., Yang, X., Li, C., Xu, X., Gotay, J. and Deng, C. X. (1998). Failure of egg cylinder elongation and mesoderm induction in mouse embryos lacking the tumor suppressor smad2. *Proc. Natl. Acad. Sci. USA* **95**, 9378-9383.

Whitman, M. (1998). Smads and early developmental signaling by the TGFbeta superfamily. *Genes Dev.* **12**, 2445-2462.

Wilkinson, D. G. (1992). *In Situ Hybridization: A Practical Approach*. London: Oxford University Press.

Wilkinson, D. G., Peters, G., Dickson, C. and McMahon, A. P. (1988). Expression of the FGF-related proto-oncogene int-2 during gastrulation and neurulation in the mouse. *EMBO J* **7**, 691-695.

Wilkinson, D. G., Bhatt, S. and Herrmann, B. G. (1990). Expression pattern of the mouse T gene and its role in mesoderm formation. *Nature* **343**, 657-659.

Wilson, V., Rashbass, P. and Beddington, R. S. P. (1993). Chimeric analysis of T (Brachyury) gene function. *Development* **117**, 1321-1331.

Winnier, G., Blessing, M., Labosky, P. A. and Hogan, B. L. M. (1995). Bone morphogenetic protein-4 is required for mesoderm formation and patterning in the mouse. *Genes Dev.* **9**, 2105-2116.

Wood, H. B. and Episkopou, V. (1999). Comparative expression of the mouse Sox1, Sox2 and Sox3 genes from pre- gastrulation to early somite stages. *Mech. Dev.* **86**, 197-201.

Wotton, D., Lo, R. S., Lee, S. and Massague, J. (1999). A Smad transcriptional corepressor. *Cell* **97**, 29-39.

Yang, J. T., Rayburn, H. and Hynes, R. O. (1995). Cell adhesion events mediated by alpha 4 integrins are essential in placental and cardiac development. *Development* **121**, 549-560.

Yang, X., Castilla, L. H., Xu, X., Li, C., Gotay, J., Weinstein, M., Liu, P. P. and Deng, C. X. (1999a). Angiogenesis defects and mesenchymal apoptosis in mice lacking SMAD5. *Development* **126**, 1571-1580.

Yang, X., Letterio, J. J., Lechleider, R. J., Chen, L., Hayman, R., Gu, H., Roberts, A. B. and Deng, C. (1999b). Targeted disruption of SMAD3 results in impaired mucosal immunity and diminished T cell responsiveness to TGF-beta. *EMBO J.* **18**, 1280-1291.

Ying, Y. and Zhao, G. Q. (2001). Cooperation of endoderm-derived BMP2 and extraembryonic ectoderm-derived BMP4 in primordial germ cell generation in the mouse. *Dev Biol* **232**, 484-492.

Ying, Y., Liu, X. M., Marble, A., Lawson, K. A. and Zhao, G. Q. (2000). Requirement of Bmp8b for the generation of primordial germ cells in the mouse. *Mol. Endocrinol.* **14**, 1053-1063.

Yoshimizu, T., Obinata, M. and Matsui, M. (2001). Stage-specific tissue and cell interactions play key roles in mouse germ cell specification. *Development* **128**, 481-490.

Zhang, H. and Bradley, A. (1996). Mice deficient for BMP2 are nonviable and have defects in amnion/chorion and cardiac development. *Development* **122**, 2977-2986.

Zhang, Y., Feng, X., We, R. and Derynck, R. (1996). Receptor-associated Mad homologues synergize as effectors of the TGF- beta response. *Nature* **383**, 168-172.

Zhu, Y., Richardson, J. A., Parada, L. F. and Graff, J. M. (1998). Smad3 mutant mice develop metastatic colorectal cancer. *Cell* **94**, 703-714.